

Dielectric Properties Characterization Based on Complementary Split-Ring Resonator

H. M. Teoh¹, S. K. Yee^{2*}

¹Research Center for Applied Electromagnetic, Faculty of Electrical and Electronic Engineering, Universiti Tun Hussein Onn Malaysia, 86400 Batu Pahat, Johor, MALAYSIA

*Corresponding Author

DOI: <https://doi.org/10.30880/emait.2020.01.01.005>

Received 9 September 2020; Accepted 30 November 2020; Available online 30 December 2020

Abstract: Material characterization method based on radio frequency and microwave measurements is highly demanded. The dielectric properties are very important for electronic circuit design, food industry, and medicine and health care. In this work, a complementary split-ring resonator (CSRR)-based sensor employed in the ground plane is proposed for dielectric measurement. This method enables the determination of both relative permittivity and relative permeability at the same time as well as simple sample preparation process. This project focuses on the design, simulation and the prediction formulae of the CSRR. This CSRR is resonating at 2.477 GHz with a quality factor of 128.91 in unloaded condition. Basically, there are shifting in the resonance frequency and the change of the quality factor when dielectric material is placed at the sensing area in separate zones. Four prediction formulas are proposed, which they are depend on the dielectric constant, real permeability, normalized resonance frequency, inverse normalized quality factor, electric loss tangent and magnetic loss tangent of the materials. These formulae are used to measure the permittivity and permeability of FR-4, Polyimide, and self-defined material. Based on the comparison, the percentage error between calculated result and reference data are 10% and 4.1% for electric and magnetic loss tangent respectively. The maximum percentage error in dielectric constant and real permeability are 4.5% and 4.29% respectively. Based on the percentage of error, it is convincing that the prediction formulas are reliable for dielectric measurement. Future work of this project should focus on verification of its actual performance through experimental measurement.

Keywords: Material characterization, dielectric measurement, permittivity, permeability, resonance frequency, quality factor

1. Introduction

Dielectric materials are substances such as glass and ceramic, that do not conduct the electric current. Different types of materials have their own dielectric constant. Thus, it is important to understand the dielectric properties in electronic circuit design [1, 2], food industry [3, 4], medicine [5, 6] and health care [7, 8]. The operation of high frequency circuits depends upon the dielectric properties of the materials. It is important to understand the properties of dielectric materials, particularly the dielectric constant and loss tangent at certain operating conditions, in order to design the high frequency circuits [9]. During operation of the high frequency circuit, high thermal conductivity is generated because it carries a high frequency signal.

Nowadays, material characterization method based on RF and microwave measurements is very important. There are various techniques for measuring dielectric properties and each of the techniques has its own advantages and limitations. Examples of techniques are transmission line, free space, resonant cavity and inductance measurement [11]. Transmission line method is a broadband technique for machinable solids, however it is limited by the effects of the air-gap. Free space method is only suitable for the samples in large and flats sheets and powders form, it is suffering from multiple reflections between the antennas and surface of the sample. Resonant cavity determines the complex

*Corresponding author: skjee@uthm.edu.my

2020 UTHM Publisher. All rights reserved.

penerbit.uthm.edu.my/ojs/index.php/ijie

permittivity of the material at selected frequency only. While inductance measurement method measures its inductance value that derives material’s magnetic permeability only.

In this project, a model of the complementary split-ring resonator (CSRR) based sensor is proposed to determine the dielectric properties such as electric permittivity and the magnetic permeability of the material under test (MUT). In order to predict the value of the dielectric constant accurately, a simulation-based database must be developed to explain the relationship between the resonance frequency, Q-factor and dielectric properties of the material. Based on the database, prediction formulas are proposed on the basis of the curve fitting methodology. The MUT is placed at the surface of the virtual CSRR sensor in CST Microwave Studio.

2. Theory of Sensing Algorithms

The resonance frequency is defined as the frequency at the maximum amplitude of the response. Basically, a simple resonator can be represented in a simple RLC circuit where its resonant frequency is given by (1)

$$f_r = \frac{1}{2\pi\sqrt{LC}} \quad (1)$$

where L and C are the inductance and capacitance. Due to the principle of perturbation, when the resonator is filled with samples that has different permittivity and permeability, the electric field and magnetic field distribution is disturbed and hence change the capacitance and inductance of the equivalent circuit. As the result, the resonance frequency and the Q-factor are altered as well. The relationship between the shift in the resonance frequency and the material dielectric properties can be expressed as (2)

$$\frac{\Delta f_r}{f_{r_unloaded}} = \frac{\int_v^0 \Delta\epsilon \mathbf{E}_1 \mathbf{E}_0 + \Delta\mu \mathbf{H}_1 \mathbf{H}_0 dv}{\int_v^0 \epsilon_o |\mathbf{E}_0|^2 + \mu_o |\mathbf{H}_0|^2 dv} \quad (2)$$

where $f_{r_unloaded}$ is the resonance frequency when the resonator is unloaded, Δf_r is the shift of resonance frequency when resonator is loaded with sample, ϵ_o is the free space permittivity, μ_o is the free space permeability, $\Delta\epsilon = \epsilon_r - 1$ represents the change in permittivity and $\Delta\mu = \mu_r - 1$ represents the change in permeability. Besides that, the \mathbf{E}_0 and \mathbf{H}_0 are the electric and magnetic fields in unloaded condition. While \mathbf{E}_1 and \mathbf{H}_1 are the disturbed fields and v is the perturbed volume. When the magnetic field is higher compare to the electric field in a resonator range, the change in the electric permittivity of the volume will not be reflected significantly on the resonance frequency, but the change in the magnetic permeability. The other way round for case when the electric field is higher.

3. Design of Complementary Split-Ring Resonator

CSRR is a compact geometrical slot embedded on the ground plane of the microwave transmission line. The defects on the ground plane are disrupting the current distribution. In this paper, the Rogers RO3003 with dielectric constant of 3, loss tangent of 0.0013, and thickness of 1.52 mm is used as the substrate. In the simulation, open air space boundary is chosen. In addition, the width of the microstrip line (top side) is set at 1.83 mm to achieve characteristic impedance of 50 ohms. Dimensions of the CSRR are given in Fig. 1.

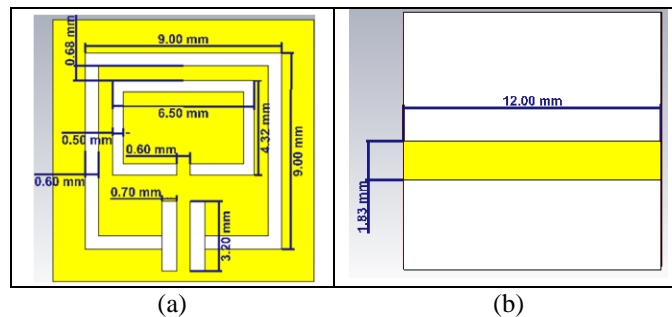


Fig. 1 - (a) Dimension of CSRR at the ground plane (bottom side); (b) microstrip line (top side)

This CSRR is proposed to determine the permittivity and permeability of the material under test. Fig. 2 shows the magnetic field, H and electric field, E distributions at the resonance frequency. Figure 2(a) shows the sensing area with high magnetic field (red color) which is suitable for detecting permeability while Fig. 2(b) indicates the sensing area for

permittivity with high intensity of electric field (red color). When placing the material under test at these areas, the strong electric field or magnetic field couple to the material under test and the variation of the permittivity and permeability can be detected [12]. Fig. 2(c) shows the resonance frequency of 2.477 GHz with a Q-factor of 128.91 in unloaded condition.

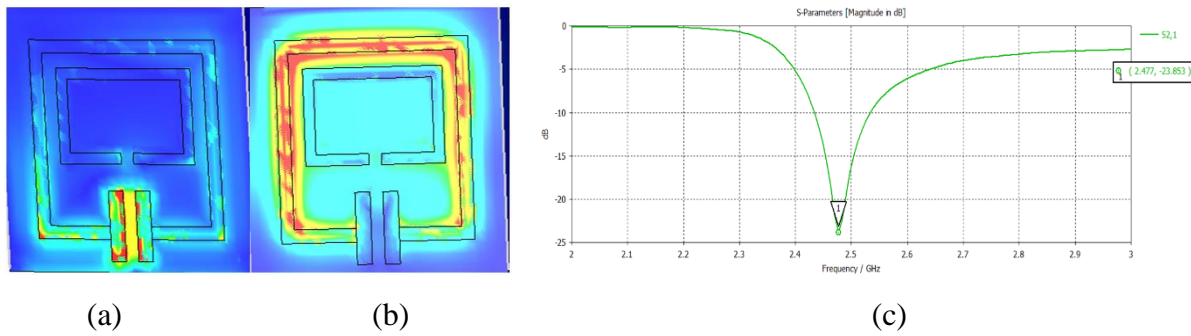


Fig. 2 - (a) Permeability sensing area with high magnetic field; (b) permittivity sensing area with high electric field; and (c) simulated S_{21} (dB) of CSRR

4. Results and Discussion

The proposed sensor is simulated using CST Microwave Studio. In the simulations, the thickness of sample is fixed to 2mm to maintain the effect of sample thickness. They are placed at their sensing area as shown in Fig. 3. The resonance frequency, f_r of CSRR is shifted when exposed to different materials that have different dielectric constant, ϵ_r . In the permittivity sensing region, the magnetic field is low, thus the effect on the f_r and Q-factor (Q) is only due to the variation of the dielectric constant, ϵ_r and electric loss tangent ($\tan \delta_e$) of samples. Figure 4(a) shows the S_{21} (dB) when ϵ_r value is ranging from 1 to 10, where its $\tan \delta_e$ is fixed at 0. While Figure 4(b) illustrates the S_{21} (dB) when the $\tan \delta_e$ is ranging from 0.01 to 0.06 where its ϵ_r is fixed at 1. It can be observed that the resonance frequency decreases from 2.477 GHz to 1.9104 GHz by increasing the ϵ_r of the sample while electric loss tangent does not shift the resonance frequency but its Q-factor.

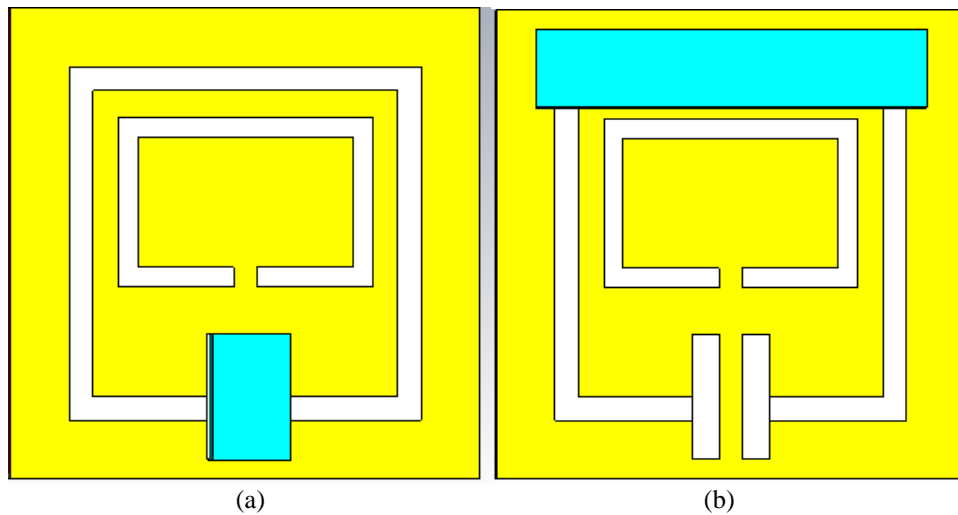
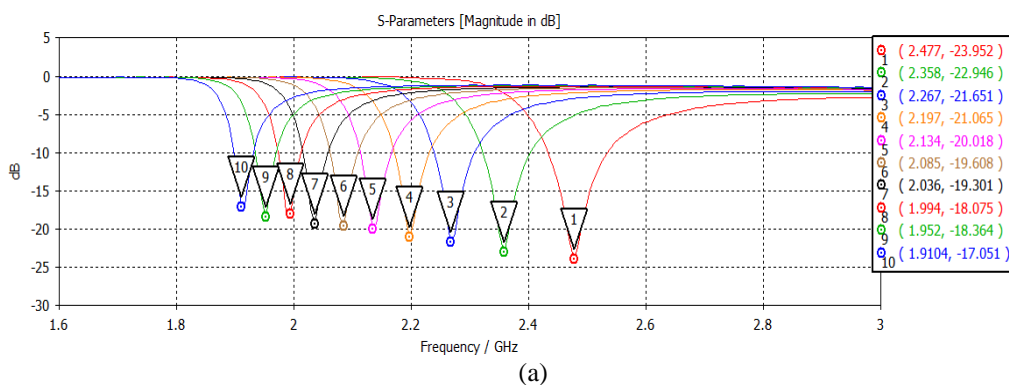
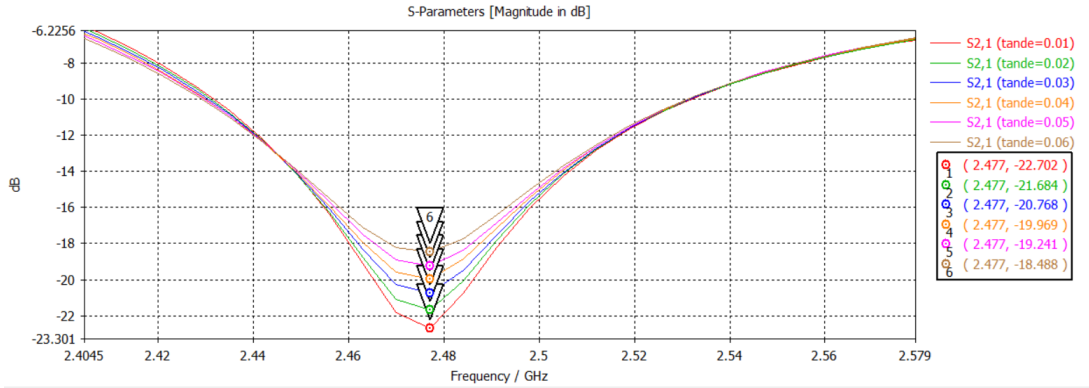


Fig. 3 - Material is placed at the sensing area for (a) permeability; (b) permittivity





(b)

Fig. 4 - S₂₁ response for different (a) ε_r (tan δ_e is fixed at 0); and (b) tan δ_e (ε_r is fixed at 1) when the MUT is placed at the permittivity sensing area

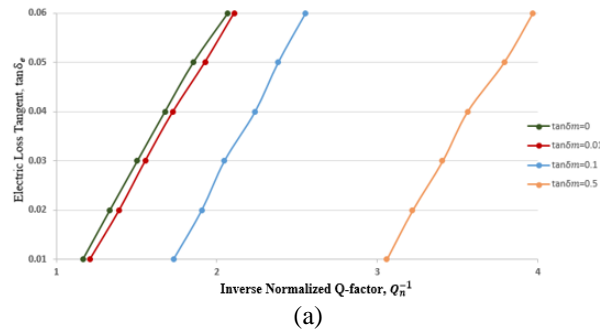
Based on the simulated results in Fig. 4 (a) the ε_r is correlated with the normalized resonance frequency (f_{rn}) by (4). The f_{rn} is the ratio of the resonance frequency of the loaded sensor (f_{rMUT}) over the resonance frequency of unloaded sensor (f_{r_unloaded}) as shown in (3).

$$f_{rn} = \frac{f_{rMUT}}{f_{r_unloaded}} \quad (3)$$

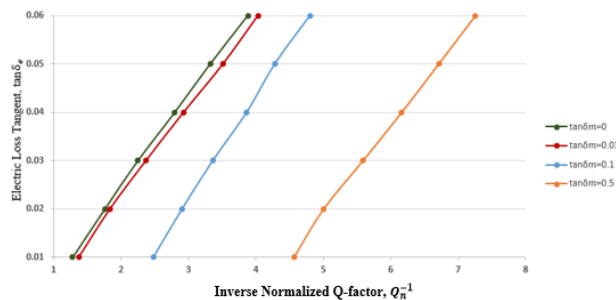
$$\epsilon_r = \frac{-3.506f_{rn}^2 + 5.552f_{rn} - 1.927}{f_{rn}^2 - 1.373f_{rn} + 0.4909} \quad (4)$$

Fig. 4(b) shows the CSRR response when different tan δ_e is defined. It is clearly observed that the change of the tan δ_e does not affect the f_r of the sample. But the magnitude of S₂₁ will increase marginally proportional to the tan δ_e. The increase in the tan δ_e from 0.01 to 0.06 has caused a decrease of Q-factor. The same finding is observed too when the ε_r = 5 and ε_r = 10 at different magnetic loss tangent. Fig. 5 shows the tan δ_e against the inverse normalized Q-factor (Q_n⁻¹) for different values of dielectric constant (ε_r=1, ε_r=5, and ε_r=10) and magnetic tangent loss (tan δ_m). The Q_n⁻¹ is the ratio of the Q-factor of the unloaded sensor (Q_{unloaded}) over that of the loaded sensor (Q_{loaded}) expressed as (5).

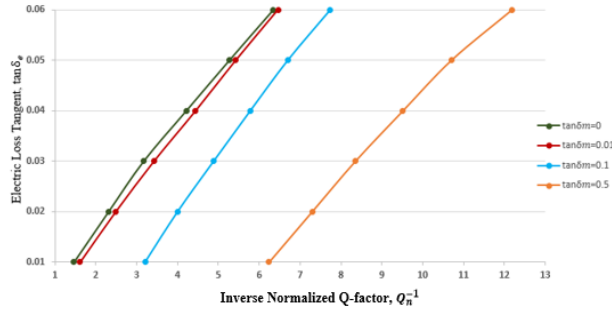
$$Q_n^{-1} = \frac{Q_{unloaded}}{Q_{loaded}} \quad (5)$$



(a)



(b)



(c)

Fig. 5 - The electric loss tangent against the inverse normalized quality factor for different values of $\tan \delta_m$ and a constant value (a) $\epsilon_r = 1$; (b) $\epsilon_r = 5$; and (c) $\epsilon_r = 10$

Based on Fig. 5, the CSRR is sensitive to the variation in ϵ_r and $\tan \delta_m$. Small change in the $\tan \delta_m$ can be detected from its Q-factor. Obviously, by increasing ϵ_r from 1 to 10, there are increment of the inversed normalized Q-factor. It can be concluded that the electric loss tangent, $\tan \delta_e$ of the MUT is affected by the values of Q_n^{-1} , $\tan \delta_m$ and ϵ_r . Thus, based on the curve fitting tool in Matlab, the general equation of that relates $\tan \delta_e$, $\tan \delta_m$ and ϵ_r can be expressed as (6)

$$\tan \delta_e = y_1 + y_2 \tan \delta_m + y_3 Q_n^{-1} + y_4 \tan \delta_m^2 + y_5 \tan \delta_m Q_n^{-1} + y_6 (Q_n^{-1})^2 \quad (6)$$

where y_1 to y_6 are functions of dielectric constant.

$$y_1 = -1.0958\epsilon_r^2 + 17.832\epsilon_r - 76.536$$

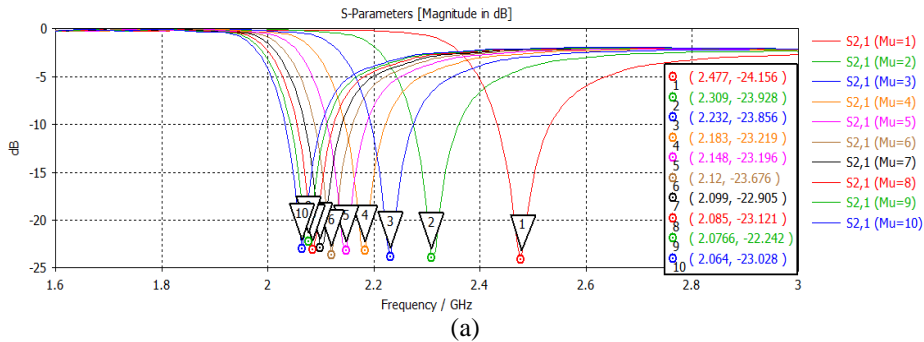
$$y_2 = -2.615\epsilon_r^2 + 46.665\epsilon_r - 387.35$$

$$y_3 = 1.0065\epsilon_r^2 - 16.542\epsilon_r + 76.945$$

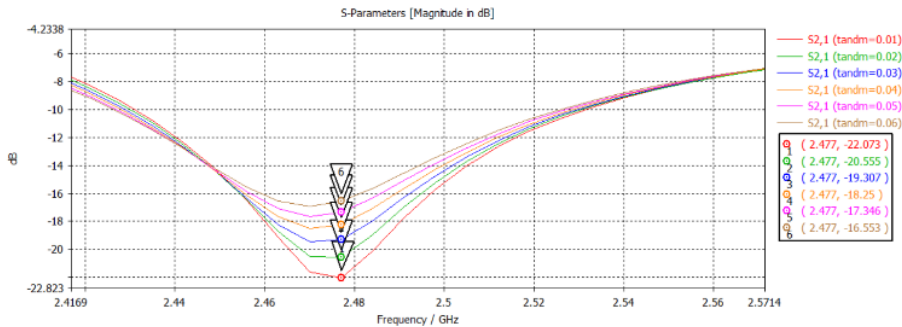
$$y_4 = -0.1906\epsilon_r^2 - 6.2817\epsilon_r + 240.77$$

$$y_5 = 0.2511\epsilon_r^2 - 3.2531\epsilon_r + 7.721$$

$$y_6 = -0.0402\epsilon_r^2 + 0.5574\epsilon_r - 1.7592$$



(a)



(b)

Fig. 6 - Sensor response for different (a) μ_r ($\tan \delta_m = 0$); and (b) $\tan \delta_m$ ($\mu_r = 1$) when the MUT is placed in the permeability sensing area

When sample with different permeability is defined at its sensing area, the resonance frequency of the resonator is shifted as well as shown in Fig. 6. Since the permittivity would not influence the sensor response at the permeability sensing area, thus, the change in the resonance frequency is purely due to the variation of the real permeability (μ_r) of the sample and magnetic loss tangent ($\tan \delta_m$). Obviously, the f_r decreases dramatically from 2.477 GHz to 2.064 GHz, by increasing the value μ_r of the sample. A fractional relationship is proposed to extract the real permeability in terms of the normalized resonance frequency is shown in (7)

$$\mu_r = \frac{-1.366f_{rn}^2 + 2.644f_{rn} - 1.233}{f_{rn}^2 - 1.569f_{rn} + 0.6151} \quad (7)$$

The simulation result as shown in Fig. 6(b) is determined by varying $\tan \delta_m$, while the value of μ_r is fixed to 1. The resonance frequency is constant and not impacted by changing the value of $\tan \delta_m$. In Fig. 7, as the $\tan \delta_m$ increases from 0.01 to 0.06 for different values of μ_r ($\mu_r=1, \mu_r=1.5$ and $\mu_r=2$), the Q-factor in each cases decreases noticeably. The inverse normalized Q-factor decreases as the value of μ_r increases. Therefore, the $\tan \delta_m$ as a function of the Q_n^{-1} and μ_r is shown in (8)

$$\tan \delta_m = (-51.52 + 35.58Q_n^{-1} + 17.72\mu_r - 2.052(Q_n^{-1})^2 + 7.841Q_n^{-1}\mu_r - 7.899\mu_r^2) \times 10^{-3} \quad (8)$$

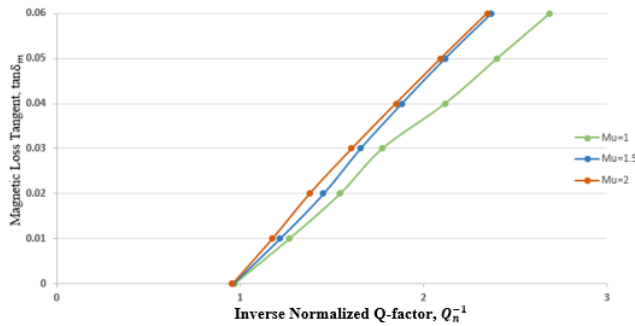


Fig. 7 - The magnetic loss tangent against the inverse normalized quality factor for different value of $\mu_r = 1, 1.5, 2$

6. Validation of Four Prediction Formula

The validity of the formulas is proven based on the selection of different materials in library of CST Microwave Studio and self-defined material (material 1) as shown in Table 1. Their relative complex permittivity (ϵ_r and $\tan \delta_e$) and relative complex permeability (μ_r and $\tan \delta_m$) are calculated based on the proposed formulations. The maximum percentage error in the dielectric constant and real permeability measurements is 4.5% and 4.29% respectively. While the maximum percentage error in the electric and magnetic loss tangent is 10% and 4.17% respectively. Based on these readings, it can be concluded that the prediction formulas are robust and reliable for predicting the dielectric properties of materials. Future works should be focused on simulation of sample properties at small step size of dielectric constant or loss tangent so that a more accurate model can be deduced.

Table 1 - Comparison of Complex Permittivity and Permeability for Different Dielectric Materials

MUT	ϵ_r		Error (%)	$\tan \delta_e$		Error (%)
	Simulation	Actual		Simulation	Actual	
FR-4	4.43	4.3	3.02	0.0256	0.025	2.4
Polyimide	3.49	3.5	0.29	0.00276	0.0027	2.2
Material 1	4.18	4	4.5	0.011	0.01	10
MUT	μ_r		Error (%)	$\tan \delta_m$		Error (%)
	Simulation	Actual		Simulation	Actual	
FR-4	1	1	0	0	0	0
Polyimide	1	1	0	0	0	0
Material 1	1.46	1.4	4.29	0.115	0.12	4.17

7. Conclusion

In this research, a technique for material characterization based on CSRR is presented. This CSRR sensor has the advantages of easy to use and ease of sample preparation. The proposed sensor is resonating at 2.477 GHz with a quality factor of 128.91. The CSRR sensor has two separate sensing zones to localize the electric and magnetic fields and these zones have been used to measure material's properties separately. By placing samples of the MUT in these sensing zones, there are changes in the resonance frequency and the quality factor of the CSRR. Based on the changes of resonance frequency and quality factor, the four electromagnetic parameters of the MUT (ϵ_r , $\tan \delta_e$, μ_r , $\tan \delta_m$) can be calculated by using the prediction formula in this research. The validation has been performed by using different materials such as FR-4, Polyimide, and self-defined material. Based on the percentage of error, it has been proven that the prediction formulas are reliable for material characterization.

Acknowledgement

The author would to thank the Research Center for Applied Electromagnetic, Faculty of Electrical and Electronic Engineering, Universiti Tun Hussein Onn Malaysia, Batu Pahat, Johor.

References

- [1] Wan, Yongbiao, et al. (2018). Natural plant materials as dielectric layer for highly sensitive flexible electronic skin. *Small* 14.35: 1801657
- [2] Hajra, Sugato, et al. (2018). Structural, dielectric and impedance characteristics of (Bi_{0.5}Na_{0.5})TiO₃-BaTiO₃ electronic system." *Journal of Alloys and Compounds* 750: 507-514
- [3] Regier, M., K. Knoerzer, and H. Schubert. (2017) Introducing microwave-assisted processing of food: Fundamentals of the technology. *The Microwave Processing of Foods*. Woodhead Publishing., 1-22
- [4] Orsat, V., G. S. V. Raghavan, and K. Krishnaswamy. (2017). Microwave technology for food processing: An overview of current and future applications. *The microwave processing of foods*. Woodhead Publishing., 100-116
- [5] Shahzad, Atif, et al. (2017). Broadband dielectric properties of adrenal gland for accurate anatomical modelling in medical applications. *2017 International Conference on Electromagnetics in Advanced Applications (ICEAA)*. IEEE
- [6] Amin, Bilal, et al. (2019). A review of the dielectric properties of the bone for low frequency medical technologies. *Biomedical Physics & Engineering Express* 5.2: 022001
- [7] Li, Changzhi, et al. *Principles and Applications of RF/microwave in Healthcare and Biosensing*. Academic Press, 2016
- [8] Gabriel, Camelia, and Azadeh Peyman. (2018). Dielectric properties of biological tissues; variation with age. *Conn's Handbook of Models for Human Aging*. Academic Press. 939-952
- [9] Sebastian, M. T., M. A. S. Silva, and A. S. B. Sombra. (2017). *Measurement of microwave dielectric properties and factors affecting them*. *Microw. Mater. Appl.* 2V Set, John Wiley & Sons, Ltd, Chichester, UK: 1e51
- [10] Janezic, Michael D., N. G. Paulter, and J. E. Blendell. (2001) Dielectric and conductor-loss characterization and measurements on electronic packaging materials. *NIST Technical note* 1520
- [11] Note, Application. (2006). *Basics of measuring the dielectric properties of materials*. Agilent Technologies: 1e31
- [12] Saadat-Safa, Maryam, et al. (2019). A CSRR-based sensor for full characterization of magneto-dielectric materials. *IEEE Transactions on Microwave Theory and Techniques* 67.2: 806-814